Supplementary Information

Slanted gold mushroom array: a switchable bi/tridirectional surface plasmon polariton splitter

Yang Shen,[ac#] Guisheng Fang,[a#] Alexander Cerjan,[b#] Zhenguo Chi,[c] Shanhui Fan*[b] and Chongjun Jin*[a]

[a]State Key Laboratory of Optoelectronic Materials and Technologies, School of Materials Science and Engineering, Sun Yat-Sen University, Guangzhou 510275, China

[b]Department of Electrical Engineering, Ginzton Laboratory, Stanford University, Stanford, CA 94305-4088, USA

[c]School of Chemistry and Engineering, Sun Yat-Sen University, Guangzhou 510275, China

1. SGMA fabrication

We fabricated the SGMA samples through an orthogonal two-beam interference lithography followed by oblique electron beam deposition. First, a clean quartz slide was treated with oxygen plasma etching for 5 minutes in order to make it hydrophilic and then a ~50-nm layer of PMMA (molecular weight: 350,000, 1.5 wt% in chlorobenzene) was spin-coated onto the slide, serving as an adherent to the photoresist pillars, and baked on a hotplate at 180℃ for 5min. After that, a layer of positive photoresist (AR-P 3740,Allresist, 14.5wt% in a thinner AR 300-12, Allresist) with thickness of 540-560 nm (owing to the fluctuation in the humidity in the lab) was spun onto the PMMA film, then baked on a hotplate at 95℃ for 90 s. The two orthogonal exposures and sequential developing were then performed to form the photoresist pillars array in square lattice. To generate a SGMA(1,1), during each

exposure the incident angle φ of the two laser beams with respect to the normal was ~21°, and the rotation angle α of the sample with respect to the plane that is perpendicular to the angle bisector formed by these two laser beams was maintained at ~6°. For SGMA(1,0) with same lattice constant in x and y directions, the (φ, α) parameters of first and second exposures were (21.3°,10°) and (20.7°,0°), respectively. For NGMA, the (φ, α) parameters are (20.7°,0°). Finally, an oblique electron beam evaporation of 5-nm nickel and 100-nm gold with the deposition direction parallel to the axis of the slanted pillars was applied to form the SGMAs.

2. FDTD simulations

We investigated the corresponding spectra and electric field distributions of gold mushroom arrays using an FDTD commercial software (FDTD solutions, Lumerical) in this paper. For the finite and infinite structures, perfectly matched layer (PML) and periodic boundary conditions were applied in both x and y axes, respectively. The mesh size in the metal region was chosen to be $6\times6\times6$ and $5\times5\times5$ nm^3 for the finite and infinite SGMAs. The collimated Gaussian beam and plane wave light source were utilized to excite the finite and infinite structures, respectively. The dielectric permittivity of bulk gold was taken from a Drude model with the permittivity at infinity ε_∞ = 9.8, the plasma frequency ω_{pl}= 1.37×10^{16} rad/s and the damping frequency $\omega_{damping}$ = 4.2725×10^{14} rad/s for both the finite and infinite structures. The refractive indices of the photoresist, PMMA and quartz were 1.61, 1.49 and 1.48, respectively. All the sizes were set according to the measured lengths in the SEM

images. We also performed FDTD simulations by using the dielectric function of gold from Johnson and Christy for reference (Supplementary Fig. S9). The calculated reflectance spectra by using dielectric function of gold based on the Drude model are found to be closer to the experimental ones.

3. Derivation of Equation (1)

Illuminated by a normally incident light, the SGMA is supposed to support waveguide modes propagating in the effective medium layer (with the effective refractive index n_{eff}) sandwiched by the upper and lower two-dimensional metal arrays, and the in-plane and out-of-plane components of wavevector satisfy

$$k_{\parallel} = \sqrt{k^2 - k_{\perp}^2},$$

where k represents the wavevector in the effective medium layer, which equals to $k = 2\pi/\lambda = 2\pi \cdot n_{eff}/\lambda_0$ with $\lambda \, and \, \lambda_0$ standing for the wavelengths in the effective layer and in vacuum, respectively. The propagating guided modes meet the Fabry-Pérot condition in out-of-plane direction, suggesting that the optical path must be an integral number of half-wavelengths, in other word, $2k_{\perp}h' = 2\pi m_z$, therefore the out-of-plane wavevector component is given as

$$k_{\perp} = m_z\pi/h'.$$

A normally incident wave fails to excite in-plane propagating guided mode in a planar dielectric waveguide because the corresponding wavevector component is missing, while in the SGMA, the reciprocal lattice vectors of the square lattice

provide the additional momentum to achieve this. Thus, the in-plane wavevector component of the guided mode in the effective medium layer can be written as

$$k_{\parallel} = \sqrt{\left(\frac{2m_x\pi}{a}\right)^2 + \left(\frac{2m_y\pi}{a}\right)^2},$$

where a is the period and m_x, m_y are integers indicating the specific orders of the reciprocal lattice vectors of the SGMA. Hence, the wavevector matching condition is derived as

$$\left(\frac{2n_{eff}}{\lambda_0}\right)^2 - \left(\frac{m_z}{h'}\right)^2 = \left(\frac{2m_x}{a}\right)^2 + \left(\frac{2m_y}{a}\right)^2.$$

4. The effects of the lattice constant, dislocation between the top and bottom gold array and waist diameter of the incident Gaussian beam on the unidirectional coupling efficiency and extinction ratio for the SGMAs

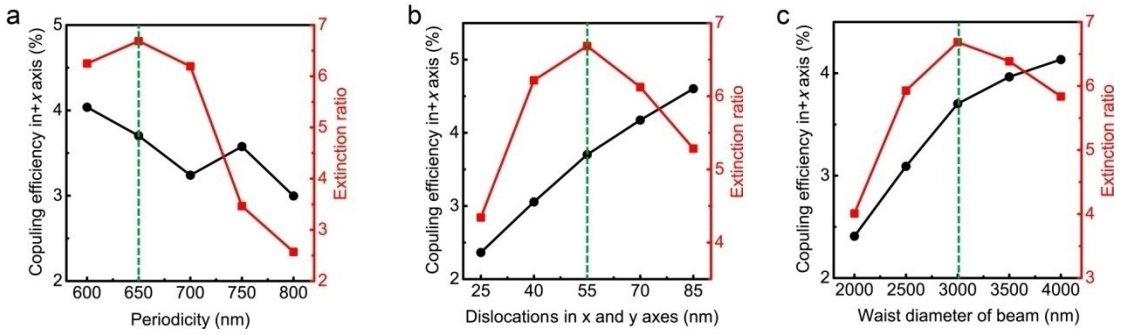

Fig. S1. The effects of the lattice constant, dislocation between the top and bottom gold arrays and waist diameter of the incident Gaussian beam on the unidirectional coupling efficiency and extinction ratio for the SGMA with 5×5 periods at the wavelengths with the largest extinction ratios. (a) Unidirectional coupling efficiency and extinction ratio as a function of the periodicity of the array. Except *a*, the other

fixed parameters are h = 550 nm, t = 100 nm, w_1 = 255 nm, w_2 = 225 nm and $\Delta x = \Delta y$ = 55 nm, D = 3000 nm, respectively; (b) Unidirectional coupling efficiency and extinction ratio as a function of the dislocation between the top and bottom arrays. Except Δx and Δy, the other fixed parameters are a = 650 nm, h = 550 nm, t = 100 nm, w_1 = 255 nm, w_2 = 225 nm and D = 3000 nm, respectively; (c) Unidirectional coupling efficiency and extinction ratio as a function of the waist diameter of the incident beam. Except D, the other fixed parameters are a = 650 nm, h = 550 nm, t = 100 nm, w_1 = 255 nm, w_2 = 225 nm and $\Delta x = \Delta y$ = 55 nm, respectively.

5. Directional coupling efficiencies and extinction ratios for the SGMAs

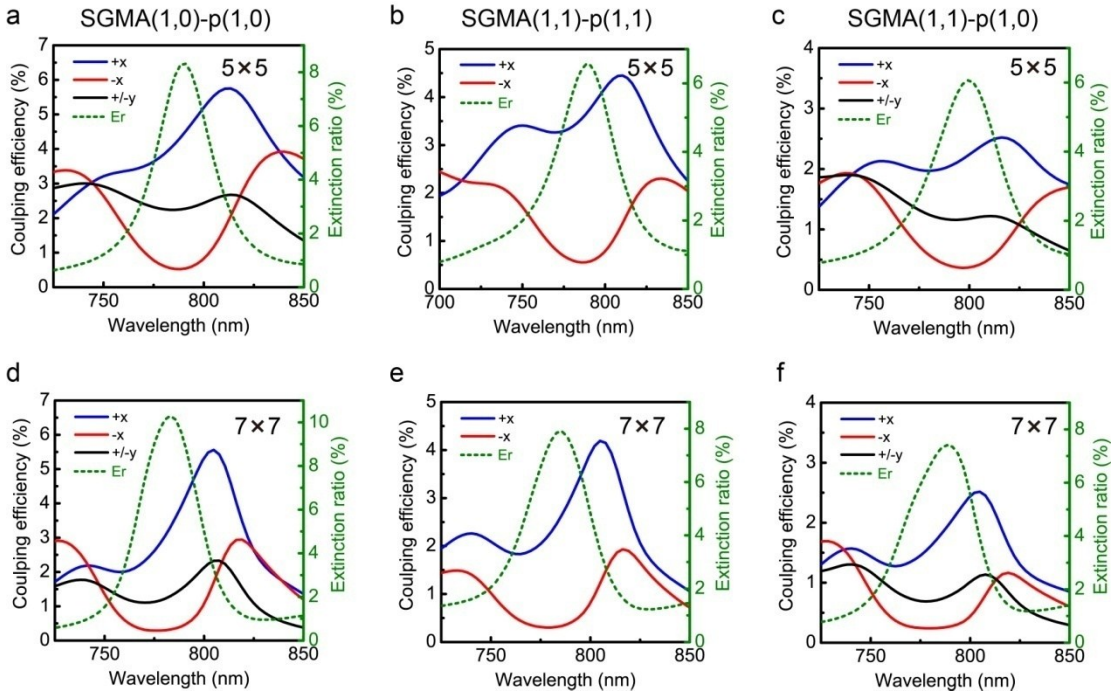

Fig. S2 Directional coupling efficiencies and extinction ratios for the three configurations of the 5×5 and 7×7 SGMAs respectively. (a,d) Calculated coupling

efficiencies (solid curves) and extinction ratios (dashed curve) of 5×5 and 7×7 SGMA(1,0) (Δx=100 nm, Δy=0 nm) under (1,0)-polarized illumination, respectively. (b,e) Calculated coupling efficiencies and extinction ratios of 5×5 and 7×7 SGMA(1,1) (Δx=55 nm, Δy=55 nm) under (1,0)-polarized illumination, respectively. (c,f) Calculated coupling efficiencies and extinction ratios of 5×5 and 7×7 SGMA(1,1) (Δx=55 nm, Δy=55 nm) under (1,1)-polarized illumination, respectively. The waist diameters of the collimated Gaussian beams in simulations were 3000 nm. The sizes of the SGMAs are a = 640 nm, h = 550 nm, t = 100 nm, w_1 = 255 nm and w_2 = 225 nm, respectively.

Table S1. The directional coupling efficiencies and extinction ratios for different configurations of SGMAs with 5×5 periods and DDMG with 5 periods.

Structure	Polarization &Wavelength	Coupling efficiency to +x direction	Coupling efficiency to -x direction	Coupling efficiency to +y direction	Coupling efficiency to -y direction	Total coupling efficiency	Extinction ratio
2D SGMA(1,1)	(1,1)@788 nm	3.65%	0.56%	3.65%	0.56%	8.42%	6.5
2D SGMA(1,1)	(1,0)@799 nm	2.22%	0.37%	1.16%	1.16%	4.91%	6.1
2D SGMA(1,0)	(1,0)@788 nm	4.52%	0.54%	2.28%	2.28%	9.62%	8.4
Quasi-1D SGMA(1,0)	(1,0)@870 nm	8.98%	0.11%	0.73%	0.73%	10.55%	81.6
1D DDMG	(1,0)@894 nm	18.30%	0.17%	-	-	18.48%	107.6

6. Schematic showing the geometry for measuring the reflectance spectrum of the NGMA/SGMAs at normal incidence

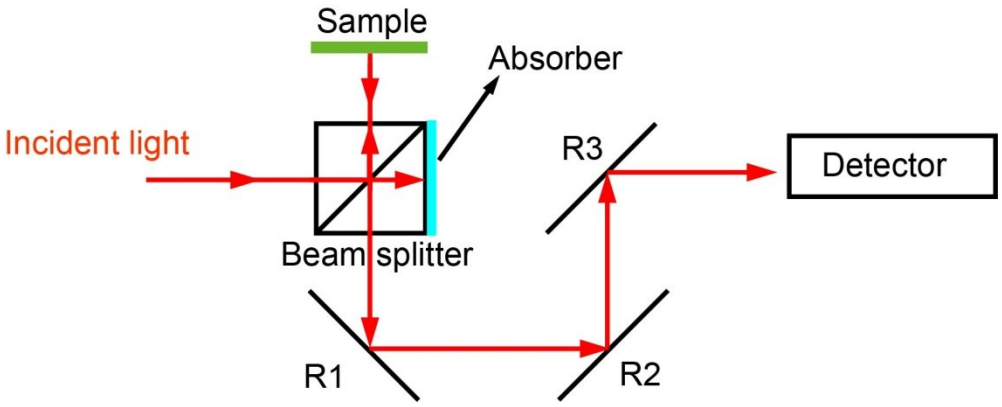

Fig. S3 Schematic showing the geometry for measuring the reflectance spectrum of the NGMA/SGMAs at normal incidence. The final reflectance spectra of the NGMA/SGMAs were corrected by dividing them with the spectrum of a silver mirror.

7. Absorption and electric field intensity distributions of the resonant modes in SGMA

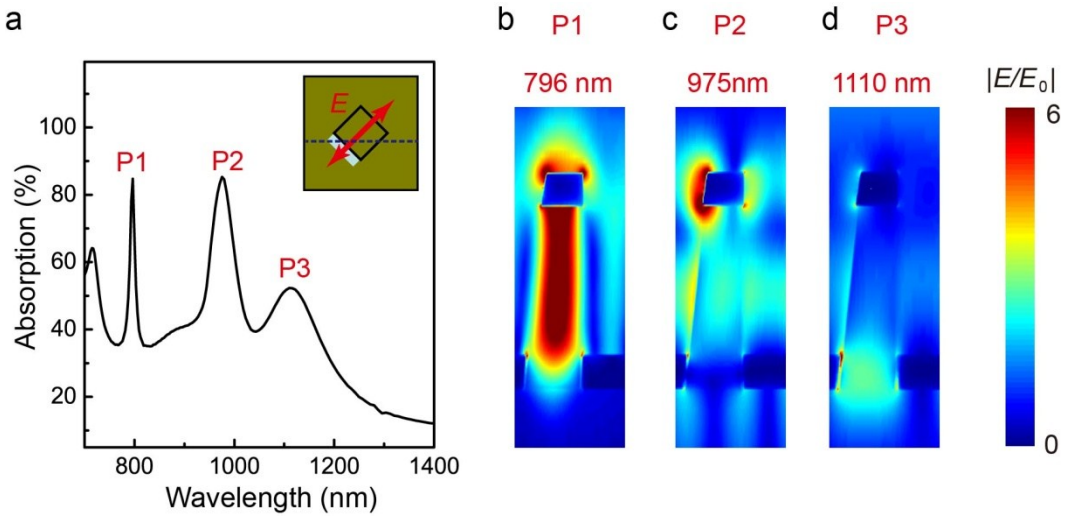

Fig. S4 Absorption and electric field intensity distributions of the resonant modes in SGMA. (a) Simulated absorption spectra of a SGMA(1,1) under normally incident light with (1,1)-polarization, as shown in inset. (b-d) Simulated electric field intensity distributions at *x*-*z* plane formed by cutting along the diagonal of the bottom square hole (indicated by the blue dashed line in inset of a) for the peaks P1, P2 and P3, respectively, at the linear scale. The sizes of the SGMA are a = 640 nm, h = 550 nm, t = 100 nm, w_1 = 255 nm, w_2 = 225 nm, Δx = 55 nm and Δy = 55 nm, respectively.

8. Origin of the red-shift of D3 for the measured reflectance spectra of the SGMAs compared to the simulated ones

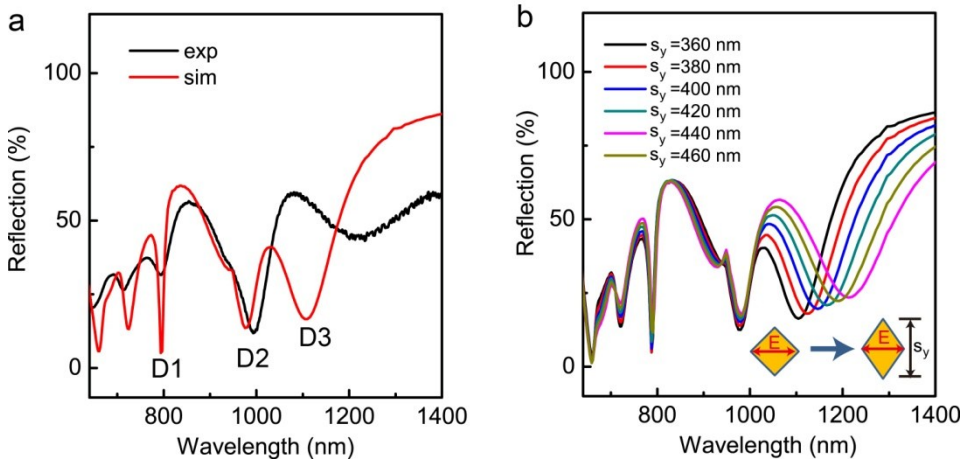

Fig. S5 Origin of the red-shift of D3 for the measured reflectance spectra compared to the simulated one. (a) Comparison of experimental and simulated reflectance spectra for a SGMA(1,0) under the normally incident illumination with (1,0)-polarization. (b) Simulated reflectance spectra of the SGMA(1,0) with varying diagonal lengths S_y of caps/holes in the direction that is perpendicular to the polarization of the incident light. The fixed parameters of the SGMAs are a = 640 nm, h = 550 nm, t = 100 nm and S_x = 360 nm, respectively.

9. Recorded images of a SGMA(1,1) under off-resonance excitations with (1,1)-polarization

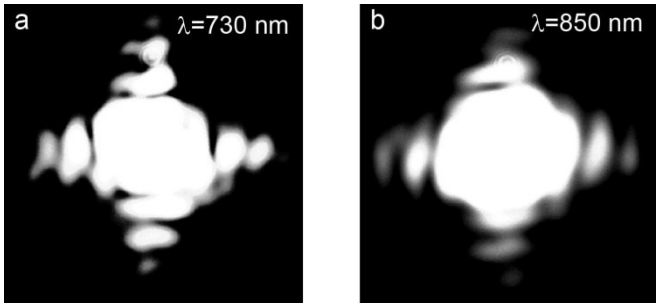

Fig. S6 Recorded images of a SGMA(1,1) under off-resonance excitations with (1,1)-polarization. (a,b) Wavelengths of the incident light are 730 and 850 nm, respectively. There is no observable unidirectional coupling effect in these two cases.

10. Simulated electric field intensity distributions at *x-y* plane (4 nm above the top surface of the bottom gold film) under some other configurations

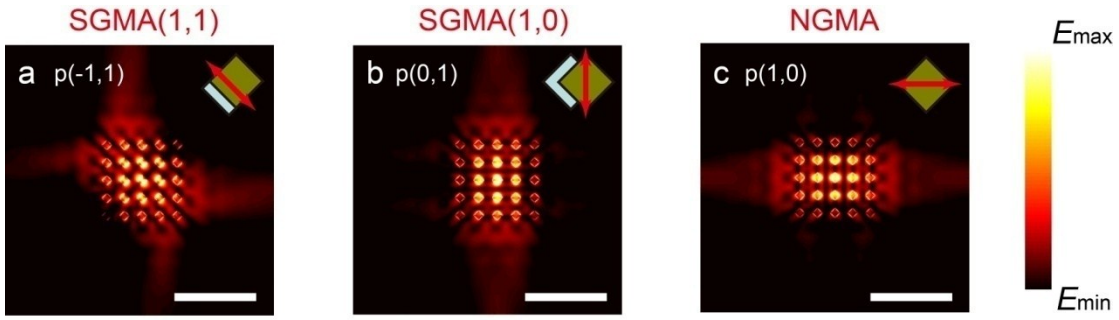

Fig. S7 Simulated electric field intensity distributions at *x*-*y* plane (4 nm above the top surface of the bottom gold film) under some other configurations (a) SGMA(1,1) (Δx = 55 nm, Δy = 55 nm) under the normally incident illumination with (-1,1)-polarization, respectively. (b) SGMA(1,0) (Δx = 100 nm, Δy = 0 nm) under the normally incident illumination with (0,1)-polarization. (c) NGMA (Δx = 0 nm, Δy = 0 nm) under the normally incident illumination with (1,0)-polarization. The sizes of the NGMA/SGMAs are a = 640 nm, h = 550 nm, t = 100 nm, w_1 = 255 nm and w_2 = 225 nm, respectively. (a-c) Scale bars, 3000 nm.

11. Experimental and simulated optical detection manners

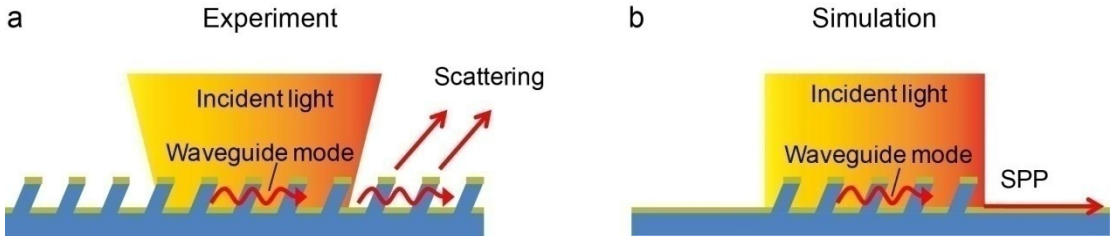

Fig. S8 Experimental and simulated optical detection manners. In experiments, a focused Gaussian beam was used to launch a unidirectional waveguide mode, a portion of which would be re-scattered to the free space during its propagation in the infinite SGMAs and was recorded by camera. While in simulations, the light source is replaced by a collimated Gaussian beam, and the unidirectional waveguide mode would be further coupled to SPP mode at the interface of air and gold film connecting the edge of SGMAs.

12. Comparison between the measured and simulated reflectance spectra of the SGMA (1,1) using various material parameters of gold

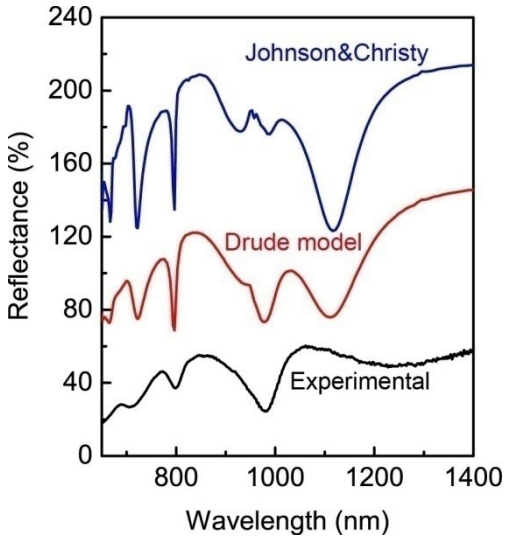

Fig. S9 Comparison between the measured and simulated reflectance spectra of the SGMA (1,1) using various material parameters of gold. The dielectric functions of gold obtained from Drude model (red curve) and from the data by Johnson and Christy (blue curve) were utilized in FDTD simulations. Evidently, the simulated result using Drude model is more in accordance with the measured one (black curve). The sizes of the SGMA(1,1) are a = 640 nm, h = 550 nm, t = 100 nm, w_1 = 255 nm, w_2 = 225 nm, Δx = 55 nm and Δy = 55 nm, respectively.